SYNTHESIS OF MULTISPECTRAL BANDS FROM HYPERSPECTRAL DATA: VALIDATION BASED ON IMAGES ACQUIRED BY AVIRIS, HYPERION, ALI, AND ETM+

Slawomir Blonski,[1] Gerald Gasser,[1] Jeffrey Russell,[1] Robert Ryan,[1] Greg Terrie,[1] and Vicki Zanoni[2]

1. INTRODUCTION

More systematic studies are needed for a better understanding of how multispectral data properties such as ground sample distance (GSD) and spatial resolution, extent and shape of spectral bands, signal-to-noise ratio (SNR), data quantization, and band-to-band registration affect performance of remote sensing imagery in real-world applications. However, because the number of available multispectral data sources is still limited, parametric studies with varying image properties are difficult to conduct. In the case of panchromatic imagery, the amount of data collected at various scales and other parameters facilitated development of the General Image Quality Equation (GIQE) that allows predicting values of GSD, edge response, and SNR necessary to detect and identify objects of interest (Leachtenauer et al., 1997). To support systematic studies of multispectral data requirements, the Applications Research Toolbox (ART) has been developed at NASA's Stennis Space Center. The ART software provides the capability to generate simulated multispectral images with predefined properties from data acquired by existing sensors with higher spatial and spectral resolution. Multiple datasets simulated with key data characteristics varied parametrically can be then evaluated by potential end-users for utility in real-world applications.

Spectral band synthesis is a key step in the process of creating a simulated multispectral image from hyperspectral data. In this step, narrow hyperspectral bands are combined into broader multispectral bands. Such an approach has been used quite often, but to the best of our knowledge accuracy of the band synthesis simulations has not been evaluated thus far. Therefore, the main goal of this paper is to provide validation of the spectral band synthesis algorithm used in the ART software. The next section contains a description of the algorithm and an example of its application. Using spectral responses of AVIRIS, Hyperion, ALI, and ETM+, the following section shows how the synthesized spectral bands compare with actual bands, and it presents an evaluation of the simulation accuracy based on results of MODTRAN modeling. In the final sections of the paper, simulated images are compared with data acquired by actual satellite sensors. First, a Landsat 7 ETM+ image is simulated using an AVIRIS hyperspectral data cube. Then, two datasets collected with the Hyperion instrument from the EO-1 satellite are used to simulate multispectral images from the ALI and ETM+ sensors.

2. SPECTRAL BAND SYNTHESIS ALGORITHM

Equations governing the spectral band synthesis process are shown here for completeness of the presentation. Although the band synthesis process has been proposed and applied previously, it is not clear if the applied formulae were the same as in the current work (Anderson et al., 2000). Band synthesis, applying an algorithm that compares more closely to the one presented here, was conducted during a cross-calibration of a satellite multispectral instrument with AVIRIS (Green and Shimada, 1997), as well as in simulations of future sensors (Esposito et al., 1999). In all the methods, each band of a multispectral image is simulated by a weighted sum of the hyperspectral image bands. Differences between the methods are in the ways the weights are determined. In the current approach, calculation of the weights is based on finding the best approximation of a multispectral response by a linear combination of the hyperspectral responses. This method is consistent with the goal of accurately modeling a sensor with a predefined spectral response.

[1] Lockheed Martin Space Operations, Stennis Space Center, Mississippi (sblonski@ssc.nasa.gov)
[2] NASA Earth Science Applications Directorate, Stennis Space Center, Mississippi

Consider a multispectral instrument (MSI) with N_{MSI} bands and a hyperspectral instrument (HSI) with N_{HSI} bands. Spectral response of the i^{th} MSI band R_i^{MSI} is defined at n wavelengths λ_k. Spectral response of the j^{th} HSI band R_j^{HSI} is also known for these wavelengths. The linear combination coefficients c_{ij} are derived by solving in the least-squares sense the following set of band-synthesis equations:

$$R_i^{MSI}(\lambda_k) = \sum_{j=1}^{N_{HSI}} c_{ij} R_j^{HSI}(\lambda_k) \quad \text{for} \quad k = 1, ..., n; \quad i = 1, ..., N_{MSI}$$

Spectral responses of existing hyperspectral instruments such as AVIRIS and Hyperion are accurately approximated with Gaussian functions. For the HSI bands with the Gaussian shape and full width at half-maximum Δ_j, the coefficients c_{ij} are used in the following weighted-sum formulae to calculate (for each pixel) spectral radiance of the synthesized multispectral image bands L_i^{MSI} from the hyperspectral radiances L_j^{HSI}:

$$L_i^{MSI} = \frac{\sum_{j=1}^{N_{HSI}} c_{ij} \Delta_j L_j^{HSI}}{\sum_{j=1}^{N_{HSI}} c_{ij} \Delta_j} \quad \text{for} \quad i = 1, ..., N_{MSI}$$

An example of the band synthesis is shown in Figure 1 for the case of Landsat 7 ETM+ Band 1 simulation from AVIRIS 1999 data. The figure also illustrates that although the synthesized bands and the actual bands closely overlap, some artifacts such as ripples at band plateaus, shoulders at band edges, and negative values outside bands do occur. Evaluation of effects of those artifacts on simulation results is presented in the following section.

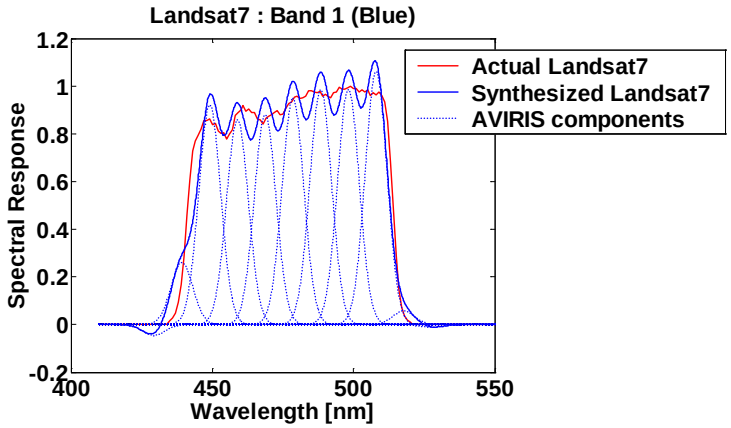

Figure 1. Comparison of actual and simulated spectral response of Landsat 7 ETM+ band 1: hyperspectral components used in the band synthesis are shown as dotted lines.

3. MODTRAN MODELING

To evaluate effects of differences between actual and synthesized spectral bands, extensive atmospheric radiative-transfer modeling was undertaken using the MODTRAN4 software (Berk et al., 1998). The calculations included the correlated-*k* option and the Isaacs approximation for the multiple scattering. About 30,000 MODTRAN calculations were conducted for each sensor: AVIRIS, Hyperion, ALI, and ETM+. The calculations were based on 1,287 surface reflectance spectra selected from the ASTER library, which comprises spectra collected at Johns Hopkins University, the NASA Jet Propulsion Laboratory (JPL), and U.S. Geological Survey (USGS) (Hook, 1999), as well as from the USGS Spectroscopy Lab collection (Clark et al., 1993). The selected spectra were measured mainly for minerals, but vegetation, soils, and man-made materials such as concrete were also included. For each reflectance spectrum, 24 MODTRAN calculations were conducted, i.e., for 6 atmospheric models combined with 4 aerosol conditions. The atmospheric models spanned a wide range of climates and seasons:

- tropical at 30°N on June 22
- tropical at 30°N on Dec. 22
- mid-latitude summer at 45°N on June 22
- mid-latitude winter at 45°N on Dec. 22
- sub-arctic summer at 60°N on June 22
- sub-arctic winter at 60°N on Dec. 22

The aerosol models were diverse as well, using the specified values of the meteorological range parameter (VIS):

- rural, VIS = 23 km
- rural, VIS = 5 km
- urban, VIS = 5 km
- tropospheric, VIS = 50 km

For all the sensors (even AVIRIS), the calculations were performed with the nadir viewing geometry from space with sensor altitude set to 100 km and ground at sea level. Solar illumination was specified by longitude of 0° and acquisition time at 10:00 UTC. To generate in-band mean spectral radiance values, convolution of the calculated atmospheric radiance spectra and the instrument spectral response functions was conducted internally within MODTRAN. The same convolution procedure was applied for the multispectral sensors, ALI and ETM+, and the hyperspectral sensors, AVIRIS and Hyperion. The calculations were based on spectral response functions obtained from existing data on spectral calibration of the instruments. Results of the MODTRAN calculations for the hyperspectral sensors were further processed with the band synthesis algorithm to simulate response of the multispectral sensors. Radiance values generated by the band synthesis were compared with those created directly in the MODTRAN modeling for the same surface reflectance and atmospheric conditions.

Synthesis of Landsat 7 ETM+ band data has been conducted from the AVIRIS and EO-1 Hyperion hyperspectral bands. The Hyperion bands were also used to synthesize the EO-1 ALI band data. Results of the band synthesis for all three cases are shown in Figure 2. In this figure, the graphs comparing the actual and synthesized spectral responses are set against scatter plots created from the MODTRAN generated data. Despite the artifacts occurring in the synthesized spectral responses, almost all the scatter plots display very high correlation between radiance values simulated from hyperspectral data by band synthesis and those generated directly in the MODTRAN modeling. Although the figure shows only data for bands 2 (green) and 4 (NIR), results for the other bands, not shown here due to limited space, are very similar to the best ones presented. The least accurate band synthesis occurs for the ETM+ band 2 simulations from Hyperion data; dispersion of points on the scatter plot suggests the possibility of 10 to 15% radiometric errors. This is in clear contrast to the very accurate simulations of the same ETM+ band from the 1999 AVIRIS data, and it is an illustration of possible effects of spectral aliasing. Although synthesis of the ALI band 4 is more challenging because of its narrow width, the respective scatter plot proves that the simulation is still quite accurate.

4. IMAGES

The AVIRIS image used for the band synthesis experiment presented in this paper was obtained from the JPL archive as a radiometrically calibrated, but not geometrically corrected, image product. The image was acquired from the high-altitude platform (ER-2) over a Maryland area at 15:35 UTC on May 11, 2000. GSD of the image was estimated to be approximately 18 m. A relatively cloud-free area of 592×656 pixels was selected from the AVIRIS image for the comparison with the Landsat 7 ETM+ image acquired near coincidentally. The ETM+ image was acquired for the Worldwide Reference System (WRS) path 15 and row 33 at 15:38 UTC on the same day as the AVIRIS image. The image was obtained from the USGS EROS Data Center (EDC) on level 0R and processed in-house to level 1G using the LPGS-lite software with the following parameters: UTM projection, GSD of 30 m, and cubic-convolution resampling. An area of 353×372 pixels, having the same extent as the AVIRIS image subset, was selected from the Landsat image.

EO-1 images selected for the presentation were obtained from NASA Goddard Space Flight Center. Both ALI and Hyperion images were only radiometrically corrected (level 1R). The first pair of the images was acquired over an Arizona area (WRS path 35, row 38) at 17:42 UTC on March 23, 2001 (day 82). The second pair was acquired over a New England area (WRS path 12, row 31) at 15:17 UTC on May 9, 2001 (day 129). Respective Landsat 7 ETM+ images were acquired one minute before the EO-1 data. Those Landsat 7 images were obtained from the EDC on level 0R as well, but they were processed only to level 1R using the LPGS-lite software. Areas of overlap between the Hyperion, ALI, and ETM+ images were selected from the images. Due to small GSD differences between the instruments, pixel sizes of the image subsets are slightly different, for example, 197×6094 pixels for Hyperion and 201×6234 pixels for ALI.

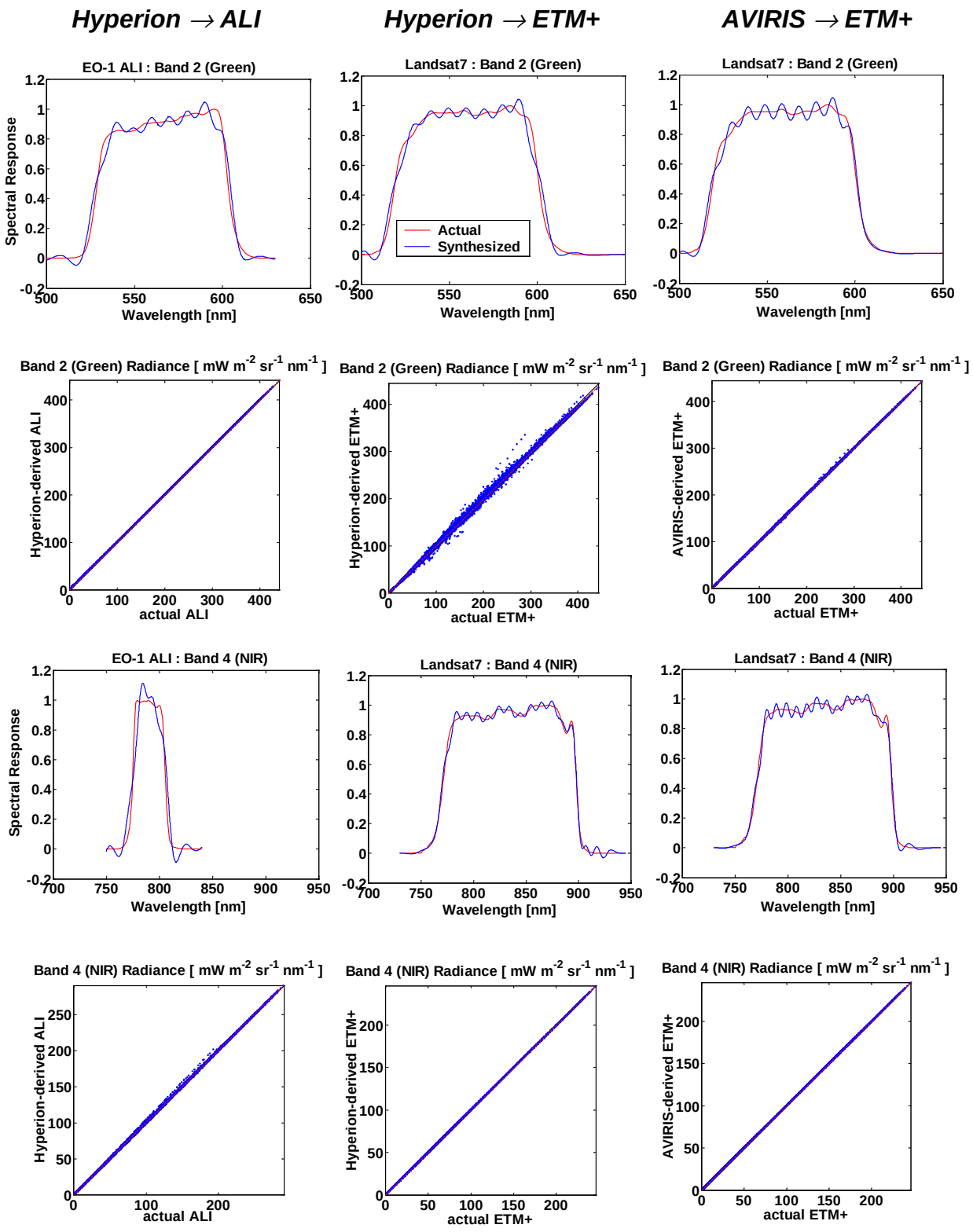

Figure 2. Comparison of spectral band synthesis results and actual spectral responses for band 2 (top row of the upper panel) and band 4 (top row of the lower panel) of the ALI and ETM+ instruments. Scatter plots created from the MODTRAN-generated data (bottom rows of both panels) show moderate effects of the band synthesis artifacts on the simulated images.

5. AVIRIS-BASED ETM+ SIMULATIONS

An image with the Landsat 7 ETM+ bands synthesized from the AVIRIS data is shown in Figure 3 together with the actual ETM+ image. Because of the GSD difference, only histograms of the images are compared in Figure 4. Despite the GSD difference, the histograms of the actual and simulated data still agree. Not only are the shapes of the histograms generally the same, but also the positions of the peaks closely match.

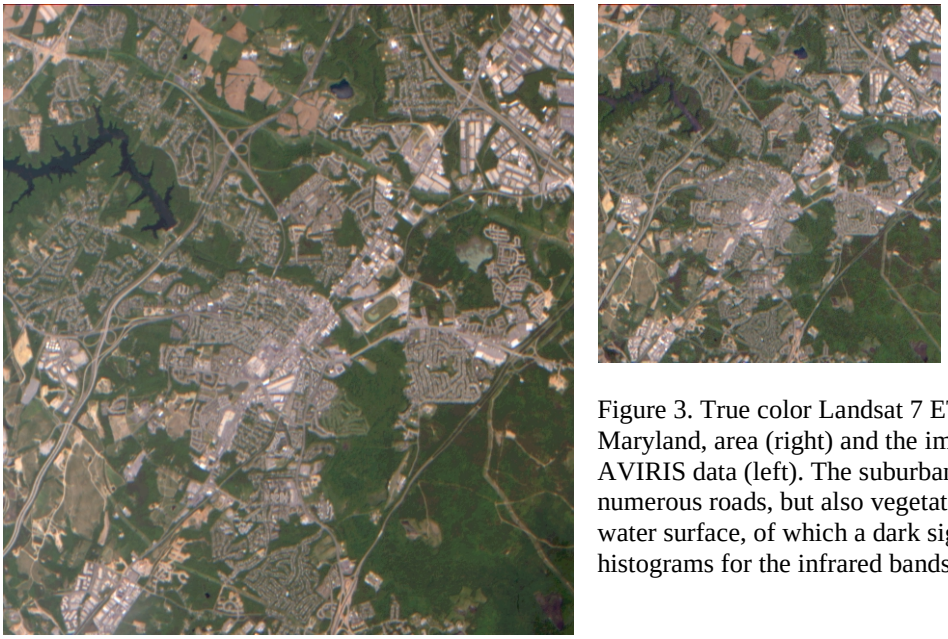

Figure 3. True color Landsat 7 ETM+ image of the Laurel, Maryland, area (right) and the image synthesized from the AVIRIS data (left). The suburban area contains not only numerous roads, but also vegetated spaces and a noticeable water surface, of which a dark signature is apparent in histograms for the infrared bands.

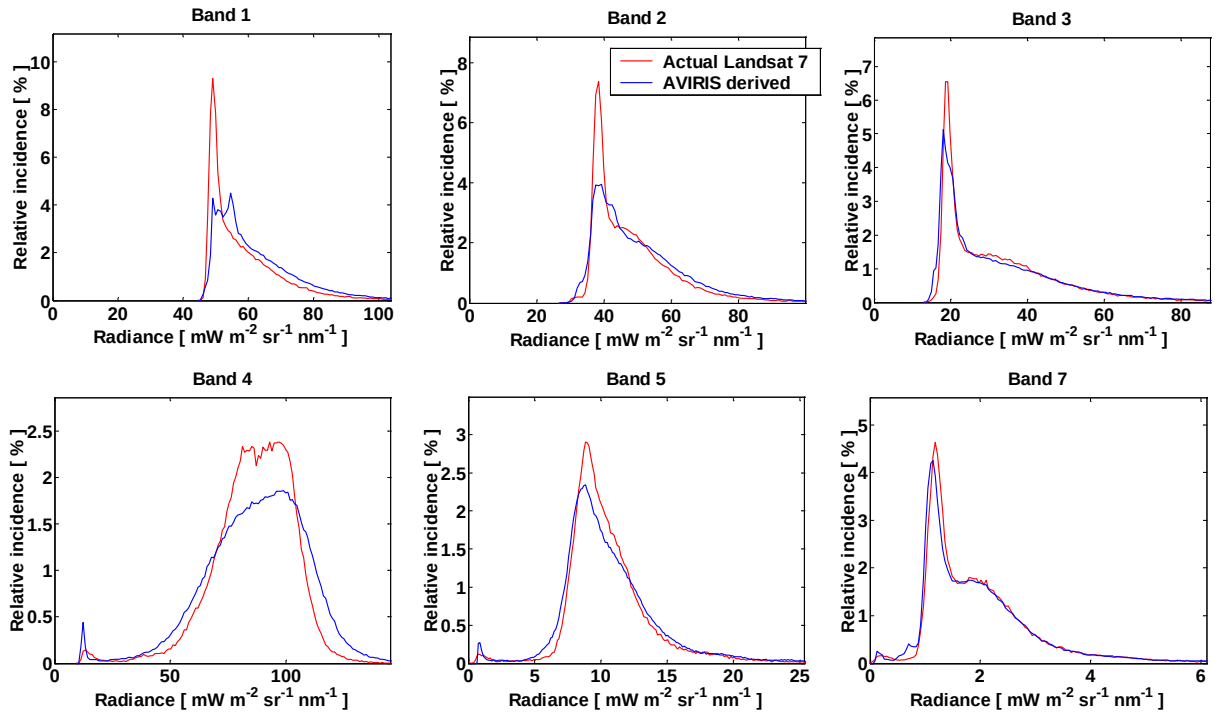

Figure 4. Histograms of radiance values for the actual Landsat 7 ETM+ image and for the image simulated by spectral band synthesis from the AVIRIS hyperspectral data.

6. HYPERION-BASED ALI AND ETM+ SIMULATIONS

EO-1 Hyperion data from Arizona and New England were used to simulate both Landsat 7 ETM+ and EO-1 ALI images. Examples of the actual and simulated images are shown in Figure 5 (New England) and Figure 6 (Arizona). The VNIR images demonstrate very good qualitative agreement between the actual and simulated data. Radiance histograms presented in Figure 7 allow for quantitative comparisons of the images. The best agreement is achieved for the simulations of bands 2 and 3 of the ALI images. Only small radiometric differences occur for the other VNIR bands. While actual ETM+ data in the VNIR bands differ a little more from the Hyperion-derived values than the ALI data, shapes of the histograms still match very closely. Hyperion-derived data diverges more significantly from the original ALI and ETM+ images in the NIR band 4, but the difference is still quite moderate. Decisively, large differences occur solely for the SWIR bands 5 and 7. Although the relative differences are close to 20-30%, the huge discrepancy observed for band 5 of the ALI image from Arizona seems to be a result of some accidental error during ground processing of that image.

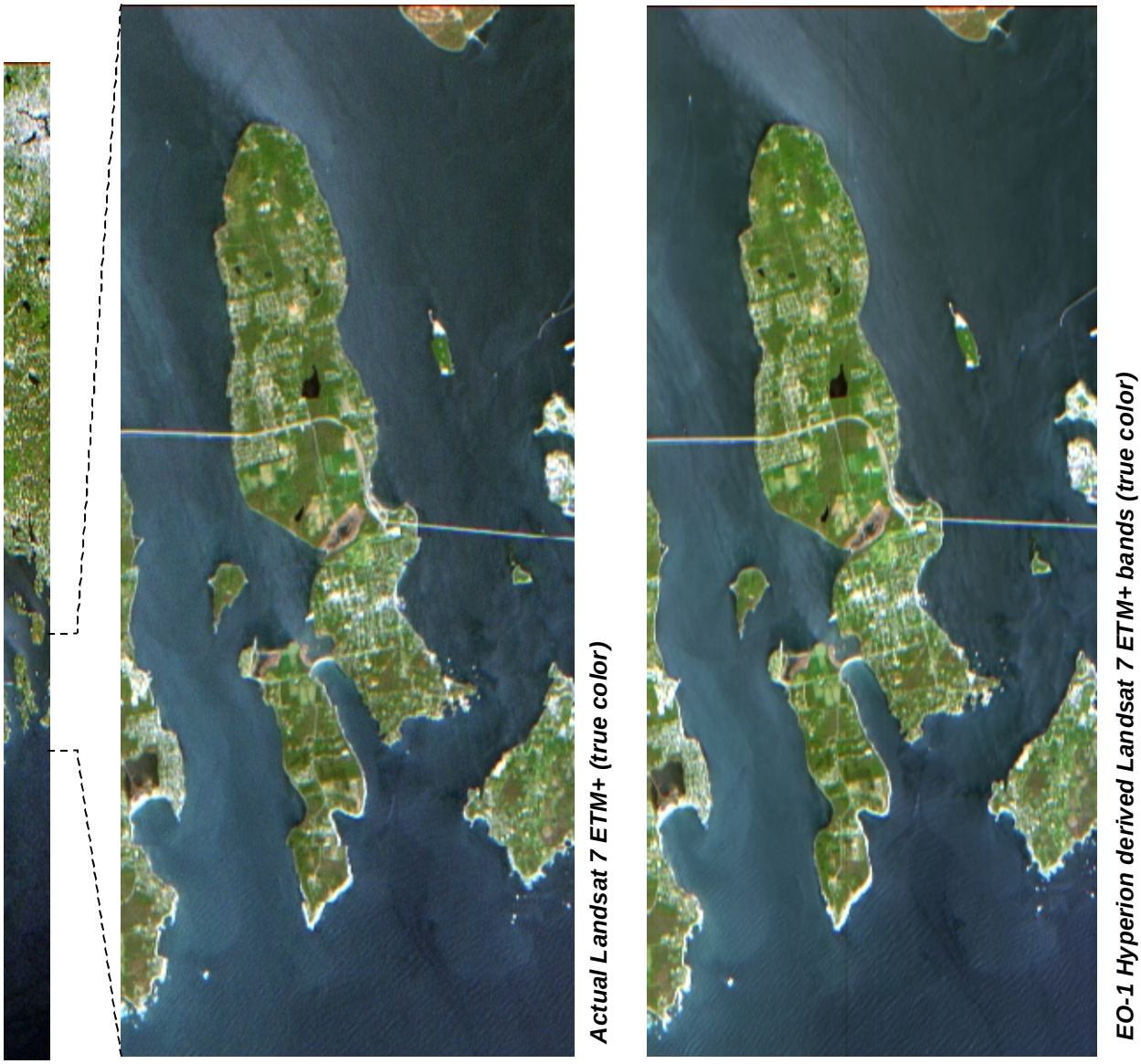

Figure 5. True color Landsat 7 ETM+ image of the New England swath (left), full-scale subsets of the ETM+ image (center) and its simulation from the EO-1 Hyperion data (right).

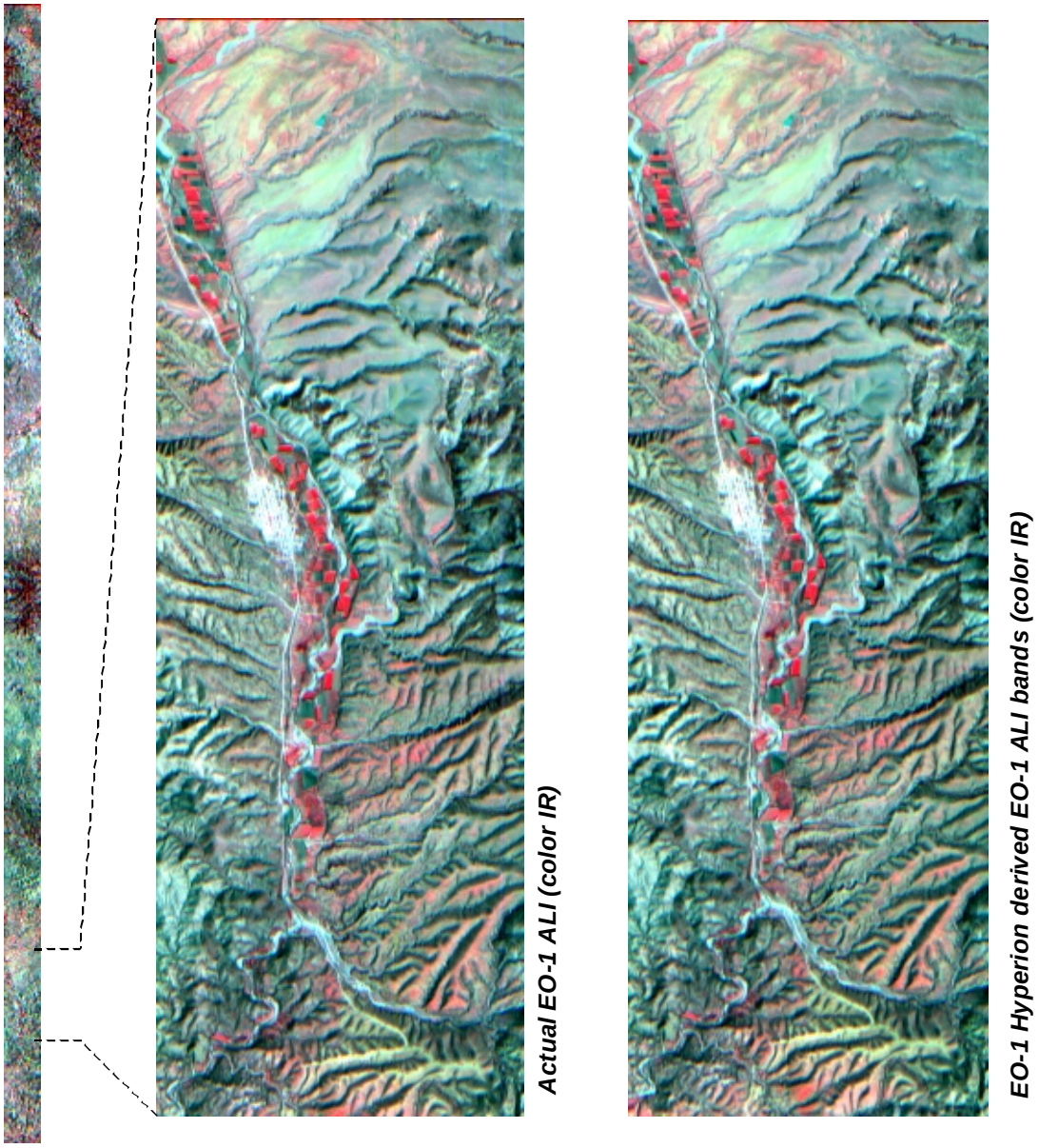

Figure 6. Color IR EO-1 ALI image of the Arizona swath (left), full-scale subsets of the ALI image (center) and its simulation from the EO-1 Hyperion data (right).

7. DISCUSSION

Overlap area of the New England images stretches from Boston, Massachusetts, to Rhode Island Sound in the Atlantic Ocean (see Figure 5). The coverage includes many urban areas, abundant vegetation (both forests and agriculture), and an extensive seawater surface. Overlap areas of the Arizona images cover mainly desert with mountains (minerals) and sparse vegetation (see Figure 6). Therefore, the two images represent quite different environments and allow for the band synthesis algorithm testing with various spectral features. Surface constituents of the Arizona images are similar to the ones used in the MODTRAN modeling. Based on the MODTRAN results presented above, a very good agreement between the actual and simulated data has been expected for the Arizona images. Although such an agreement occurs only for some spectral bands, these results and those from the AVIRIS-based simulations fully validate the presented band synthesis method.

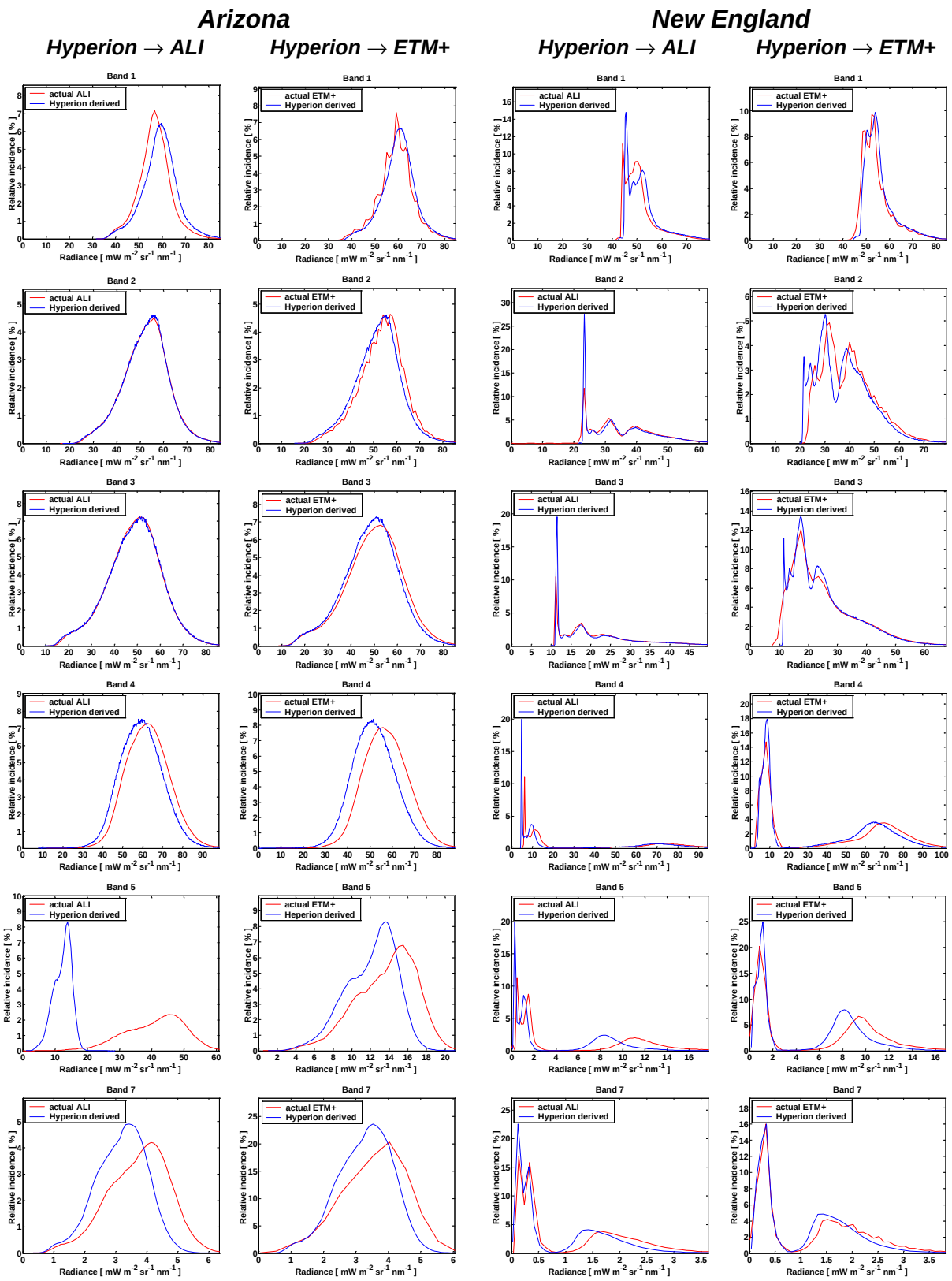

Figure 7. Histograms of radiance values for the actual EO-1 ALI and Landsat 7 ETM+ image as well as for the respective images simulated by spectral band synthesis from the Hyperion hyperspectral data.

Differences observed for the other spectral bands do not contradict the band synthesis method, but only suggest that radiometric calibration of the sensors needs to be improved. Similar results have been reported by others (Jarecke et al., 2001; Barry and Ong, 2001).

The simulations of the Landsat 7 ETM+ image using AVIRIS data acquired near-coincidently (within minutes of each other) from a high-altitude aircraft show that a very satisfactory radiometric agreement can be achieved even without applying corrections for effects of atmospheric radiative transfer processes occurring above the airplane altitude. However, in most cases the corrections will need to be applied to account for differences in viewing geometry, solar illumination, and atmospheric conditions. This becomes especially important when data from a hyperspectral instrument acquiring images from a low-altitude aircraft are to be used in modeling of satellite multispectral sensors.

8. CONCLUSIONS

A spectral band synthesis algorithm for simulations of multispectral images from hyperspectral data has been formulated and implemented in the Applications Research Toolbox software package. High correlation achieved between the simulated images and the data acquired near-coincidentally by actual remote sensing instruments has validated the algorithm. Validation has been supported by results of MODTRAN modeling conducted with an extensive set of surface reflectance spectra and atmospheric conditions. The modeling has also shown that band synthesis may be less accurate, in some cases, due to spectral aliasing. Nevertheless, the band synthesis algorithm can be effectively applied in modeling of multispectral sensors in the remote sensing applications research and development area. The same algorithm can be used as well for cross-calibration of hyperspectral and multispectral instruments (e.g., EO-1 Hyperion and ALI vs. Landsat 7 ETM+).

9. ACKNOWLEDGEMENTS

Discussions with Amanda Warner, formerly of LMSO -- Stennis Programs, and her help with the selection of AVIRIS and EO-1 images are greatly appreciated. This research was supported by the NASA Earth Science Applications Directorate under contract number NAS 13-650 at the John C. Stennis Space Center, Mississippi.

10. REFERENCES

Anderson, D.S., B. Keaffaber, and R. Wasky, 2000, “Simulation of MSI Imagery from HIS Data,” in *Algorithms for Multispectral, Hyperspectral, and Ultraspectral Imagery VI*, S.S. Shen and M.R. Descour, eds., Proc. SPIE, vol. 4049, pp. 76-81.

Barry, P. and L. Ong, 2001, “Comparison of ALI, Hyperion, and Landsat Data,” EO-1 Hyperion and Advanced Land Imager (ALI) Data Users Workshop, Baltimore, Maryland, November 28-29, 2001 (available on-line at http://eo1.gsfc.nasa.gov/)

Berk, A., L.S. Bernstein, G.P. Anderson, P.K. Acharya, D.C. Robertson, J.H. Chetwynd, and S.M. Adler-Golden, 1998, “MODTRAN Cloud and Multiple Scattering Upgrades with Application to AVIRIS,” Remote Sens. Environ., vol. 65, pp. 367-375.

Clark, R.N., G.A. Swayze, A.J. Gallagher, T.V.V. King, and W.M. Calvin, 1993, “The U. S. Geological Survey, Digital Spectral Library: Version 1: 0.2 to 3.0 microns,” U.S. Geological Survey Open File Report 93-592, 1340 pages.

Esposito, E.S.C., T. Krug, and R.O. Green, 1999, “Simulation of the Spectral Bands of the CCD and WFI Cameras of the CBERS Satellite Using AVIRIS Data,” in Summaries of the Eight JPL Airborne Earth Science Workshop, R.O. Green, ed., JPL Publication 99-17, pp. 93-102.

Green, R.O. and M. Shimada, 1997, “On-Orbit Calibration of a Multispectral Satellite Sensor Using a High Altitude Airborne Imaging Spectrometer,” Adv. Space Res., vol. 19, no. 9, pp. 1387-1398.

Hook, S.J., 1999, “ASTER Spectral Library,” Jet Propulsion Laboratory, California Institute of Technology, CD-ROM.

Jarecke, P.J., P. Barry, J. Pearlman, and B.L. Markham, 2001, “Aggregation of Hyperion Hyperspectral Spectral Bands into Landsat-7 ETM+ Spectral Bands,” in *Imaging Spectrometry VII*, M.R. Descour and S.S. Shen, eds., Proc. SPIE, vol. 4480, pp. 259-263.

Leachtenauer, J.C., W. Malila, J. Irvine, L. Colburn, and N. Salvaggio, 1997, “General Image-Quality Equation: GIQE,” Appl. Opt., vol. 36, no. 32, pp. 8322-8328.